

J. F. Deux
P. Malzy
N. Paragios
G. Bassez
A. Luciani
P. Zerbib
F. Roudot-Thoraval
A. Vignaud
H. Kobeiter
A. Rahmouni

Assessment of calf muscle contraction by diffusion tensor imaging

Received: 2 November 2007
Revised: 26 March 2008
Accepted: 30 March 2008
Published online: 8 May 2008
© European Society of Radiology 2008

J. F. Deux (✉) · A. Luciani · P. Zerbib ·
H. Kobeiter · A. Rahmouni
Service d'Imagerie Médicale,
Centre Hospitalo-Universitaire H. Mondor,
Assistance Publique-Hôpitaux de Paris,
INSERM UMR 7054,
41 av Mal de Lattre de Tassigny,
94000 Créteil, France
e-mail: jean-francois.deux@hmn.aphp.fr
Tel.: +33-1-49812631
Fax: +33-1-49814612

P. Malzy
Service d'Imagerie Médicale,
Centre Hospitalo-Universitaire Lariboisière,
Assistance Publique-Hôpitaux de Paris,
Paris, France

N. Paragios
Ecole Centrale de Paris,
Chatenay Malabris, France

G. Bassez
Service des Maladies Neuro-Musculaires,
Centre Hospitalo-Universitaire H. Mondor,
Assistance Publique-Hôpitaux de Paris,
Créteil, France

F. Roudot-Thoraval
Centre d'Investigation Clinique,
Centre Hospitalo-Universitaire H. Mondor,
Assistance Publique-Hôpitaux de Paris,
Créteil, France

A. Vignaud
Siemens Medical Division,
Paris, France

Abstract The goal of this study was to assess the changes of water diffusion during contraction and elongation of calf muscles using diffusion tensor (DT) MRI in normal volunteers. Twenty volunteers (mean age, 29 ± 4 years) underwent DT MRI examination of the right calf. Echo planar imaging sequence was performed at rest, during dorsal flexion and during plantar flexion. The three eigenvalues (λ_1 , λ_2 , and λ_3), apparent diffusion

coefficient (ADC) and fractional anisotropy (FA) of the diffusion tensor were calculated for medial gastrocnemius (mGM) and tibialis anterior (TA). A fiber tractography was performed on both muscles. Non-parametric Wilcoxon and Mann Whitney tests were used for statistical evaluation. At rest, λ_1 , λ_2 and ADC of mGM were higher than their counterparts of TA ($P < 0.01$). During dorsal flexion, the three eigenvalues and ADC of TA significantly increased ($P < 0.05$) as their counterparts of mGM slightly decreased ($P = \text{NS}$). Opposite variations were detected during plantar flexion of the foot. Visual analysis evidenced a relationship between 3D representations of MRI fibers and physiological state of muscles. Contraction of calf muscles produces changes in DT parameters, which are related to the physiological state of the muscle.

Keywords Diffusion tensor imaging · MRI · Skeletal muscle

Introduction

The theoretical basis of diffusion tensor (DT) MRI is that cell membranes and other structures constrain water diffusion in tissues leading to an anisotropic diffusion [1, 2]. Water movement can be evaluated by determining the three orthogonal directions of water diffusion, called eigenvectors, and their intensities, called eigenvalues. From the three eigenvalues (λ_1 , λ_2 and λ_3), parameters such as fractional anisotropy (FA) or apparent diffusion coefficients (ADC) can be calculated to evaluate the

character of water diffusion in a voxel. DT MRI probes muscle tissue at a microscopic scale and can provide information about the structure of skeletal lower muscles [3]. Thus, many studies have demonstrated that anatomically the first eigenvalue represents the diffusion along the main direction of fiber muscle [4–6]. In addition, it has been suggested that the second and the third eigenvalue could represent the diffusion of water within the endomyosium and throughout the fiber radius, respectively [7, 8]. Other anatomic features of muscle such as physiological cross-sectional area, fiber length and pennation angle of

fiber muscle can be obtained with DT MRI [4]. These studies have all been performed in the rest position. Limited works have studied the skeletal muscle function by diffusion imaging. It has been reported that ADC increased with muscle exercise [9, 10]. Studying rat tibialis anterior, Van Donkelaar modeled muscle deformations in numerical simulations of skeletal muscle contractions [11]. Potential applications of muscle DT MRI could extend to the study of structural changes after muscle contraction and could be a new technique for studying muscle contraction impairment. The aim of our study was to test if water diffusion changes can be detected by DT MRI performed at rest and during contraction in two opposite functional calf muscles (medial gastrocnemius muscle and tibialis anterior) in normal volunteers.

Materials and methods

Population characteristics

The study protocol was approved by the local ethics committee, and written informed consent was obtained from all subjects. Twenty normal subjects, ten women and ten men, volunteered to participate in this study. Height and weight were measured for each individual. The body mass index (BMI) was calculated for each subject. The main results are reported in Table 1.

Acquisition protocol

All MRI examinations were performed on a 1.5-T MRI system (Symphony, Siemens, Erlangen, Germany) using a standard transmitter/receiver extremity knee coil positioned on the right calf. The rest position of the foot was obtained by padding the calf in neutral position. A T1-weighted TSE sequence was performed on the calf at rest in the transversal and sagittal orientation with the following parameters: FOV=23 cm, matrix 512×256, pixel size=0.4×0.8 mm², number of slices: 20, slice thickness=6 mm, TE/TR=15/465 ms, Bw=130 Hz/px, acquisition time=2 min 3 s.

Echo planar imaging (EPI) sequence weighted in diffusion was performed on the same location to get the DT MRI data with the following parameters: transversal orientation, b=0 s/cm² and 450 s/cm², TE/TR=

104/3,600 ms, Bw=1,395 Hz/px, FOV=23×23 cm, matrix 128×128, pixel size=1.8×1.8 mm², number of slices=20, slice thickness=6 mm, 3 averages, acquisition time=2 min 26 s. Twelve direction-probing gradients were applied. The EPI sequence was performed three times on calf muscles: at rest, during a dorsal flexion of the foot and during a plantar flexion of the foot. The volunteers were asked to actively perform a plantar or dorsal flexion of the foot during the image acquisition.

DT MRI processing and fiber tracking

Axial T1-weighted images were used to find the maximal cross-sectional area of the calf (Fig. 1). A DT MRI software (Massachusetts General Hospital DTI TaskCard software, Boston, MA) was used to calculate the three eigenvalues ($\lambda_1, \lambda_2, \lambda_3$) and the corresponding eigenvectors (e1, e2, e3) for each pixel of the slice. From the three eigenvalues, the following parameters were calculated:

- the apparent diffusion coefficient (ADC) defined as follows:

$$ADC = (\lambda_1 + \lambda_2 + \lambda_3)/3$$

- the fractional anisotropy (FA) defined as follows:

$$FA = \sqrt{\frac{3 \sum_i (\lambda_i - \bar{\lambda})^2}{2 \sum_i \lambda_i^2}}$$

Parametric maps of eigenvalues, ADC (Fig. 1b) and FA, were obtained.

At the maximal cross-sectional area of the calf, a manual delineation was used to produce the boundaries of the medial gastrocnemius (mGM) and the tibialis anterior (TA) on the T1-weighted sequence (Fig. 1a). We used these boundaries to delineate mGM and TA on the EPI image performed at the same level (Fig. 1b). The pixels included inside the boundaries of the mGM and TA represented the seed region of interest that was used for the DT tractography. From the seed region, the fibers were determined through successive local search according to the dominant direction of the diffusion tensors.

The algorithms used for fiber tracking are based on previous reports [12, 13]. The search was performed both towards a proximal and a distal direction from the seedpoints. An integration step of 0.3 voxel was used. A minimal FA of 0.1 and a maximal angle change of 10° per integration step were used as the stop criteria. Tracking was continued until the stop criteria were satisfied. The DT fiber tractography of mGM and TA was performed three times for each patient on the DT images acquired at rest,

Table 1 Population characteristics of volunteers

	Men	Women	P
Age	33.6±3	26.8±2	NS
Height (m)	1.76±0.05	1.69±0.07	<0.01
Weight (kg)	70.9±12	60.3±7.9	<0.01
BMI (kg/m ²)	22.9±5	21.8±3	NS

Data are expressed as mean ± standard deviations of the mean

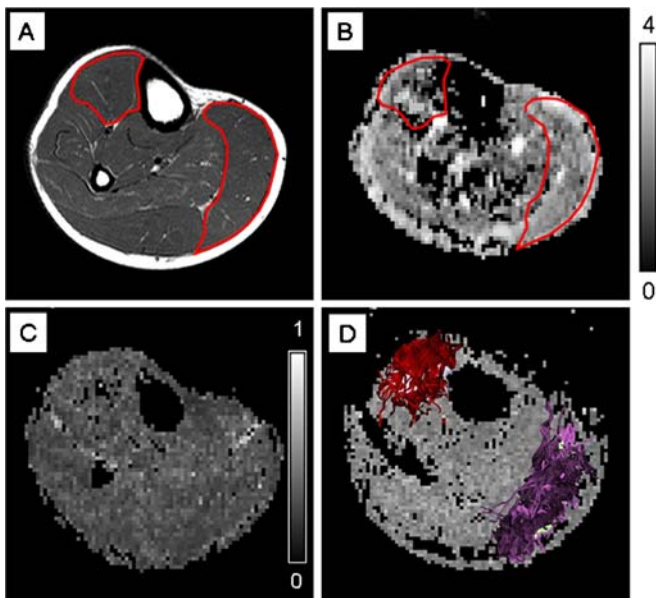


Fig. 1 Axial images of the calf of a 25-year-old volunteer. T1-weighted image located at the maximal cross-sectional area of the calf. Red lines indicate the boundaries of medial gastrocnemius (mGM) and anterior tibialis (AT) (a). Gray scale parametric maps of ADC ($\times 10^{-3} \text{ mm}^2 \cdot \text{s}^{-1}$) (b) and FA ($\times 10^{-3} \text{ mm}^2 \cdot \text{s}^{-1}$) (c) at the same level. Upper view of the tractography analysis for mGM and TA (d). DT fibers of TA are red, and DT fibers of mGM are purple (the color of the fibers is random)

during dorsal and during plantar flexion of the foot. The number of fibers within each muscle was automatically calculated by the DT MRI software at the end of the tractography. The number of fibers per pixel was calculated for each muscle by dividing the total of number of DT fibers calculated by the software for each muscle by the number of seedpoints.

Visual analysis

3D images of fibers were analyzed independently by two radiologists, blinded to the position of the foot during

acquisition of images. Visual analysis was based on fiber orientation. The physicians classified the images of one muscle according to the parallelism of fibers: class A when fibers were parallel (considered as elongation), class B when fibers were non parallel (considered as contraction) and class C for intermediate state (considered as rest). The analysis was performed sequentially in two sessions: (1) both mGM and TA were analyzed simultaneously on 3D DT images and (2) isolated mGM and isolated TA were analyzed independently on 3D DT images.

Statistical analysis

The data presented for the volunteer population and DT MRI parameter analysis are expressed as mean values \pm standard error of the mean (SEM). Non-parametric Wilcoxon and Mann Whitney tests were used for statistical evaluation. For 3D images analysis, the agreement between real anatomical position of the foot and classification of the physicians was determined by calculating Cohen's kappa coefficient. Kappa values of 0.81–1.00 correspond to near-perfect agreement.

Results

Population study

Male subjects were statistically taller and heavier than female. No statistical difference in age or BMI was found between the male and female volunteers. The main results are reported in Table 1.

DT MRI parameters

Values of λ_1 , λ_2 , λ_3 , ADC and FA are reported in Table 2 both for mGM and TA.

Table 2 Values of the three eigenvalues, FA and ADC ($\times 10^{-3} \text{ mm}^2 \cdot \text{s}^{-1}$) for mGM and TA, at rest, during dorsal flexion and during plantar flexion

	λ_1	λ_2	λ_3	FA	ADC
mGM					
Rest	2.39 \pm 0.12	1.71 \pm 0.12	1.19 \pm 0.16	0.34 \pm 0.04	1.76 \pm 0.12
Dorsal flexion (passive elongation)	2.44 \pm 0.19	1.66 \pm 0.14	1.07 \pm 0.13	0.40 \pm 0.03	1.72 \pm 0.14
Plantar flexion (contraction)	2.57 \pm 0.21	1.92 \pm 0.18	1.35 \pm 0.17	0.31 \pm 0.04	1.95 \pm 0.18
TA					
Rest	2.36 \pm 0.16	1.55 \pm 0.15	0.92 \pm 0.22	0.43 \pm 0.05	1.62 \pm 0.15
Dorsal flexion (contraction)	2.53 \pm 0.19	1.75 \pm 0.17	1.13 \pm 0.20	0.38 \pm 0.06	1.81 \pm 0.17
Plantar flexion (passive elongation)	2.52 \pm 0.21	1.69 \pm 0.18	1.07 \pm 0.19	0.41 \pm 0.04	1.76 \pm 0.19

Data are expressed as mean \pm standard deviations of the mean

Comparison of DT MRI parameters of calf muscles at rest

For both muscles we noticed a significant reduction of eigenvalues from λ_1 to λ_3 ($\lambda_1 > \lambda_2 > \lambda_3$). No significant difference was observed between mGM and TA for λ_1 ($P=0.3$) at rest. The second, the third eigenvalues and ADC of mGM were significantly higher compared to their counterparts of TA at rest ($P<0.01$ and $P<0.001$, respectively). In addition, FA was statistically lower for mGM compared to TA ($P<0.0001$).

Variation of DT MRI parameters of calf muscles from rest to dorsal flexion of the foot

During dorsal flexion of the foot (i.e., contraction of TA and elongation of mGM), we noticed that DT MRI parameters of mGM and TA exhibited opposite variations (Fig. 2).

The three eigenvalues of TA significantly increased (respectively, by 7%, 11% and 19%; $P<0.005$) leading to a significant decrease of FA by 11% ($P<0.005$) and a significant increase of ADC (+10%, $P<0.005$). Conversely, during dorsal flexion of the foot, the second and the third

eigenvalues of mGM decreased [respectively, by 4% ($P=NS$) and 10% ($P<0.005$)] as the first eigenvalue slightly increased (+2%, $P=NS$). These variations induced a significant increase of FA by 14% ($P<0.0005$). ADC of mGM decreased, but in a non-significant manner (from 2%) (Fig. 2).

Variation of DT MRI parameters of muscles from dorsal flexion to plantar flexion of the foot

From dorsal to plantar flexion of the foot (i.e., elongation of TA and contraction of mGM), DT MRI parameters of muscles exhibited opposite variations (Fig. 2).

The three eigenvalues of mGM increased by 5% ($P=NS$), 13% ($P<0.005$) and 21% ($P<0.005$), leading to a significant decrease of FA ($P<0.05$) and a significant increase of ADC ($P<0.05$). Conversely, the three eigenvalues of TA slightly decreased (respectively by 1, 4 and 6%, $P=NS$), leading to a non-significant decrease of ADC ($P=NS$) and a slight increase of FA ($P=NS$) (Fig. 2).

Comparison of DT MRI parameters of mGM and TA at the same state of contraction

DT MRI parameters were analyzed when both muscles were in contraction (i.e., during dorsal flexion of the foot for TA and during plantar flexion of the foot for mGM). We noticed that differences noted at rest persist in contraction: the second and the third eigenvalues of mGM (respectively, 1.92 ± 0.18 and 1.35 ± 0.17) were statistically higher than their counterparts of TA (respectively, 1.75 ± 0.17 and 1.13 ± 0.20 , $P<0.03$). In addition FA of mGM (0.31 ± 0.04) was statistically lower than FA of TA (0.38 ± 0.06 , $P<0.0006$). No significant difference of DT MRI parameters was noticed between muscles when they were in elongation.

DT fiber tractography

The total number of fibers detected on DT fiber tractography was significantly higher for mGM than TA ($3,114 \pm 177$ and $2,148 \pm 129$, respectively, $P<0.0001$) in all volunteers. The number of fibers per pixel in mGM and in TA exhibited no significant difference (7.76 ± 0.04 and 7.77 ± 0.02 , respectively, $P=0.7$).

Visual analysis of 3D representations of both muscles has led to an excellent relationship between DT image classification and the real anatomical position of the foot (Cohen's kappa coefficient: 0.95 and 0.85 for radiologist 1 and 2, respectively). Examples of 3D images of fibers of mGM and TA are shown in Fig. 3. When muscles were analyzed independently (Figs. 4 and 5), the analysis of the DT images of mGM produced excellent results in terms of classification of the physiological state of the muscle

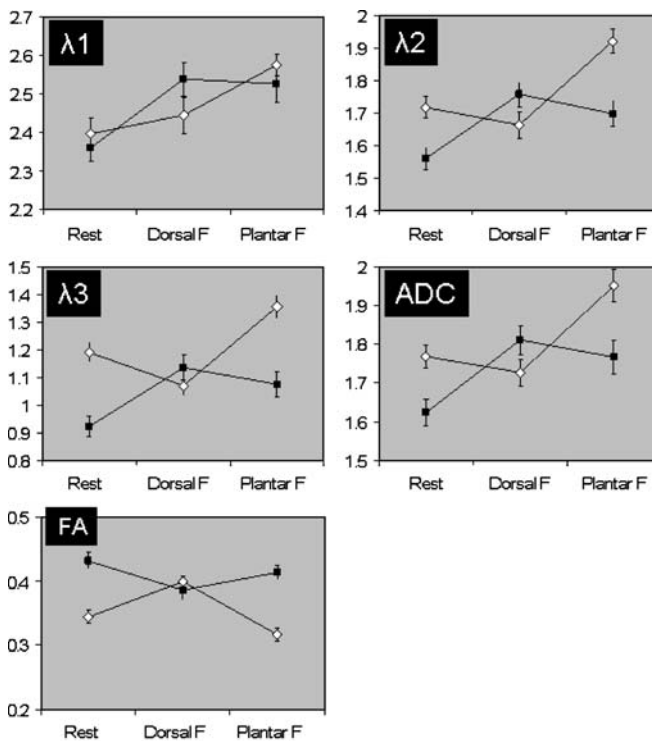


Fig. 2 Changes in MR indexes before and after movement of the foot. Data are mean values ($\times 10^{-3} \text{ mm}^2 \cdot \text{s}^{-1}$) of the three eigenvalues, ADC and FA for mGM (\diamond) and TA (\blacksquare), at rest, during dorsal flexion and during plantar flexion of the foot. Error bars represent standard deviation. These graphs show the crossing of the DT parameters when opposite muscles contract

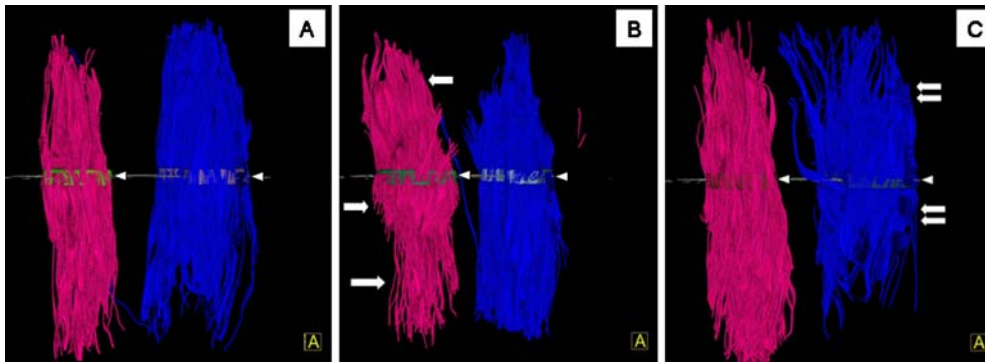


Fig. 3 3D representations of anterior views of MRI fibers of mGM (blue fibers) and TA (red fibers) obtained from DT fiber tractography, at rest (a), during dorsal (b) and during plantar flexion (c) of the foot for the same volunteer. Color structure at the middle part of the fibers (arrowhead) represents the seedpoints. During dorsal flexion of the foot, tractography evidenced a loss of parallelism of DT fibers of TA (arrows) in comparison to rest position, reflecting muscle contraction. In the same manner, loss of

parallelism of MRI fibers of mGM is observed on tractography after plantar flexion of the foot (c, double arrows) that induces a contraction of mGM (a). These results illustrate opposite variations of MRI fibers of mGM and TA, function of foot movement and state of contraction of muscles. Modifications of MRI fibers between rest and elongation of muscles (dorsal flexion for mGM and plantar flexion for TA) are less evident

(Cohen's kappa coefficient: 0.95 and 0.82 for radiologist 1 and 2, respectively). Nevertheless, for TA the relationship was poor (Cohen's kappa coefficient: 0.20 and 0.18 for radiologist 1 and 2, respectively).

Comparison of DT MRI parameters between genders

For mGM no significant difference of DT MRI parameters was observed between the gender at rest, during dorsal flexion and plantar flexion. For TA we noticed that the first eigenvalue was statistically higher ($P < 0.05$) for females when compared to males at rest position. No other significant differences were noted. Total number of fibers of mGM was significantly higher in men ($3,494 \pm 212$) than in women ($2,504 \pm 212$) ($P < 0.05$). No significant difference of total number of fibers of TA was noted between men ($2,142 \pm 161$) and women ($2,154 \pm 212$) ($P = 0.7$). A significant increase of number of fibers per pixel was noted for both muscles at rest for male (7.87 ± 0.03 and 7.83 ± 0.03 , respectively, for mGM and TA) in comparison to female (7.64 ± 0.07 and 7.71 ± 0.03 , respectively, for mGM and TA, $P < 0.05$).

Discussion

The main contribution of this study was to demonstrate the changes of DT MRI parameters when contraction of muscles occurs. A relationship was found between DT MRI parameters and the functional state of the muscle. Furthermore, we have reported that 3D models of fibers obtained with MR fiber tractography can be used to accurately identify the state of contraction of two opposite muscles of the calf for normal volunteers. To the best of our knowledge, such results have never previously been reported.

Several studies have reported that the processing of muscle DT MRI can lead to measurements that coincide with histological characteristics of skeletal muscles [6, 14, 15]. Leg and calf muscles were studied at rest by DT MRI in animal models [3], in human volunteers [16] or after human skeletal muscle injury [17]. In this work we decided to evaluate the modifications of DT parameters induced by contraction or elongation of muscle in vivo. We have considered two calf muscles that belong to two opposite functional muscle groups based on their action on the ankle: mGM is predominantly used for extending the foot, whereas TA acts in foot dorsiflexion. Our hypothesis was that differences in DT parameters may be detected during

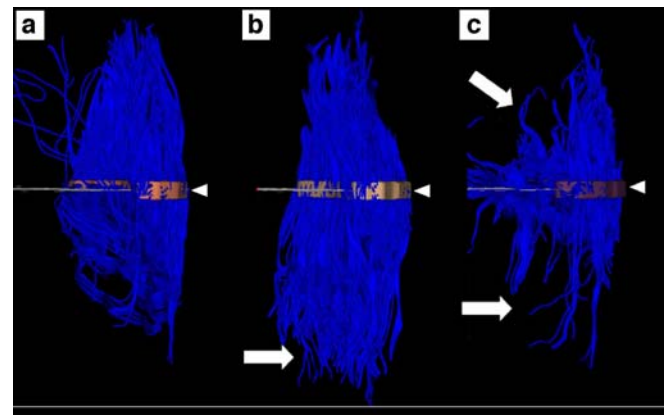


Fig. 4 3D representations of anterior views of DT fibers of mGM at rest (a), during dorsal (b) and during plantar flexion (c) of the foot for the same volunteer. Color structure at the middle part of the fibers (arrowhead) represented the seedpoints. During dorsal flexion of the foot, DT MRI detects an increase of parallelism of fibers (b, arrow) in comparison to rest position, reflecting muscle elongation. A loss of parallelism of MRI fibers is observed after plantar flexion of the foot (c, arrows) because of contraction of mGM that reduces anisotropic factor of muscle

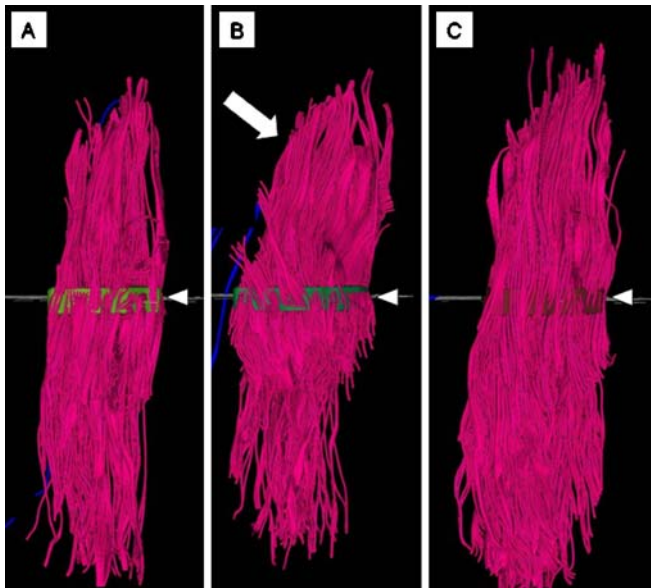


Fig. 5 3D representations of anterior views of MRI fibers of TA at rest (a), during dorsal (b) and during plantar flexion (c) of the foot for the same volunteer. Color structure at the middle part of the fibers (arrowhead) represented the seedpoints. During dorsal flexion of the foot, DT MRI detects a loss of parallelism of MRI fibers (b, arrow) in comparison to rest position, reflecting muscle contraction. No difference is seen after plantar flexion of the foot (c) that induces an elongation of TA

active dorsal and plantar flexion of the foot due to opposite behavior of mGM and TA.

It has been previously reported there is a geometric relation between the eigenvectors calculated with DT MRI and the fiber muscle architecture when observed *in vivo*. In the myocardium, Tseng et al. [8] have demonstrated that the three eigenvalues, λ_1 , λ_2 and λ_3 , correspond to the direction along the long axis of the fibers, parallel to the myocardial sheets and normal to the sheets. In skeletal muscles, many studies have reported that the first eigenvalue (λ_1) represents the diffusion transport of water along the main axis of the fiber [4, 16]. In our study, eigenvalues of mGM and TA at rest were similar [7] or slightly higher [14] than those previously reported. We noticed that λ_2 and λ_3 of TA were statistically lower at rest than their counterparts in mGM. According to these results, it has been previously reported that TA had the smallest λ_3 among all calf muscles in human volunteers at rest [14]. The differences of diffusive properties that we report at rest may be linked to structural differences between muscles, as suggested by Galban et al. [7, 14]. Based on previously report of Tseng et al. [8], he proposed that λ_2 could represent the diffusion of water within the endomysium, and λ_3 could represent the cross section of the fiber. Thus, he reported in normal volunteers that diffusive properties of muscle can help to distinguish functional differences between muscle and demonstrated a strong relation between λ_3 and the physiological cross-section area

(PCSA) of muscles [7, 14]. Anatomically, variations in the average PCSA have been already reported in hindlimb muscles of rats [18].

Few studies have considered muscle contraction with DT MRI. Van Donkelarr et al. [11] have reported that numerical fibers obtained after DT tractography can be used directly in numerical simulations of skeletal muscle contractions. In the present work, we detected significant variations of DT MRI parameters when muscle state changes from rest to contraction, during active movement of the foot. Opposite variations of DT MRI parameters that we detected for mGM and TA during foot movement enhance the hypothesis of a relationship between DT MRI parameters and the physiological state of the muscles. When the muscle's state changed from rest (or contraction) to elongation, variations of DT MRI parameters were detected, but were not significant. Contraction of the muscle induced most likely more important anatomical changes, such as modifications of shape and length, than does elongation, and our population may be too small to detect significant variations.

During muscle contraction, we noticed a significant increase of the three eigenvalues, both for mGM and TA. These variations were more pronounced for λ_3 and, in a least manner for λ_2 , leading to a decrease of the global anisotropy of water diffusion in the muscles. To our knowledge, this result has never been reported before. Variations of eigenvectors that we noticed must be interpreted with caution because of lack of anatomical correlations. Nevertheless, some points can be underlined. First, variations of λ_1 between contraction and passive elongation of muscles were weak and non-significant (except during contraction of TA), suggesting that modification of physiological state of the muscle did not influence diffusion of water along the main direction of the fibers. Second, λ_3 , and in a less significant manner λ_2 , exhibited the most important variations during muscle contraction (in contrast to λ_1), indicating that modifications of water diffusion during contraction occurred essentially in other directions than the main fiber direction.

Physiologically, muscle contraction is induced by a shortening of fibers in a constant volume, resulting in an increase of muscle diameter [19], and probably an increase of fiber diameter and muscle subunits. Thus, we think that the significant increase of λ_3 that we noticed during contraction (and in a less significant manner the decrease of λ_3 during passive elongation) for both muscles reinforces the hypothesis of a relationship between fiber radius and the third eigenvalue, as already proposed by Galban et al. at rest [7, 14]. Changes of the second eigenvalue that we observed during contraction and passive elongation may suggest modifications of endomysium, a complex structure including vessels, nerves and collagen fibers [20]. However, this hypothesis cannot be yet validated without anatomical correlations.

Finally, we used MR tractography to generate 3D representations of fibers. The total number of fibers detected with tractography was significantly higher in mGM than TA, mainly because of differences in cross-sectional areas between muscles. Considering differences between males and females, we noticed that a higher number of fibers per pixel was present in men compared to women for both muscles ($P < 0.05$). Skeletal muscle distribution is influenced by gender [21]. Studying skeletal muscle mass and distribution by MRI, Janssen et al. [22] have reported that skeletal muscle mass in men was 36% greater than in women and that this difference remained after controlling for gender differences in body weight and height. Galban et al. [14] using DT MRI have reported that a larger volume fraction of skeletal muscle seems to be devoted to fibers in men than in women. These results may suggest that men have a higher anatomical density of muscle fibers. We acknowledge that the standard deviation of the mean density in both men and women is close to 1%, which could be related to the homogeneity of the patients included in this initial study. These results should be confirmed in ongoing studies including patients of different age and constitution.

Our results reveal also that MRI fibers can be used to accurately separate rest and contraction of two opposite

muscles. Nevertheless, it must be underlined that loss of parallelism of fibers observed on 3D images during muscle contraction does not reflect a real anatomical change of direction of anatomic fiber present in muscles in vivo. Physiologically, in vivo, a shortening of anatomic muscle fibers is observed during contraction, but their direction remains globally constant. The reduction of muscle anisotropy during contraction might have affected the efficiency of the fiber tracking software, leading it to erroneously jump between pixels of adjacent slices. These mistakes of connection may have created misregistered unparallel fibers.

In conclusion, we report that DT parameters are related to the physiological state of contraction of two opposite skeletal muscles of the calf. The variations of the DT MRI parameters of muscles from rest to contraction or from rest to elongation could be a new tool to evaluate muscle function. Additionally, this method could be used as an accurate, quantitative and reproducible technique to monitor muscle function impairment. Current investigations are underway in a population of patients with degenerative muscle disorders to evaluate the potential clinical relevance of this technique.

References

1. Basser PJ, Jones DK (2002) Diffusion-tensor MRI: theory, experimental design and data analysis—a technical review. *NMR Biomed* 15:456–467
2. Mattiello J, Basser PJ, Le Bihan D (1997) The b matrix in diffusion tensor echo-planar imaging. *Magn Reson Med* 37:292–300
3. Damon BM, Ding Z, Anderson AW, Freyer AS, Gore JC (2002) Validation of diffusion tensor MRI-based muscle fiber tracking. *Magn Reson Med* 48:97–104
4. Heemskerk AM, Strijkers GJ, Vilanova A, Drost MR, Nicolay K (2005) Determination of mouse skeletal muscle architecture using three-dimensional diffusion tensor imaging. *Magn Reson Med* 53:1333–1340
5. Sinha U, Yao L (2002) In vivo diffusion tensor imaging of human calf muscle. *J Magn Reson Imaging* 15:87–95
6. van Doorn A, Bovendeerd PH, Nicolay K, Drost MR, Janssen JD (1996) Determination of muscle fibre orientation using diffusion-weighted MRI. *Eur J Morphol* 34:5–10
7. Galban CJ, Maderwald S, Uffmann K, de Greiff A, Ladd ME (2004) Diffusive sensitivity to muscle architecture: a magnetic resonance diffusion tensor imaging study of the human calf. *Eur J Appl Physiol* 93:253–262
8. Tseng WY, Wedeen VJ, Reese TG, Smith RN, Halpern EF (2003) Diffusion tensor MRI of myocardial fibers and sheets: correspondence with visible cut-face texture. *J Magn Reson Imaging* 17:31–42
9. Morvan D, Leroy-Willig A (1995) Simultaneous measurements of diffusion and transverse relaxation in exercising skeletal muscle. *Magn Reson Imaging* 13:943–948
10. Nygren AT, Kaijser L (2002) Water exchange induced by unilateral exercise in active and inactive skeletal muscles. *J Appl Physiol* 93:1716–1722
11. Van Donkelaar CC, Kretzers LJ, Bovendeerd PH, Lataster LM, Nicolay K, Janssen JD et al (1999) Diffusion tensor imaging in biomechanical studies of skeletal muscle function. *J Anat* 194(Pt 1):79–88
12. Basser PJ, Pajevic S, Pierpaoli C, Duda J, Aldroubi A (2000) In vivo fiber tractography using DT-MRI data. *Magn Reson Med* 44:625–632
13. Mori S, van Zijl PC (2002) Fiber tracking: principles and strategies—a technical review. *NMR Biomed* 15:468–480
14. Galban CJ, Maderwald S, Uffmann K, Ladd ME (2005) A diffusion tensor imaging analysis of gender differences in water diffusivity within human skeletal muscle. *NMR Biomed* 18:489–498
15. Heemskerk AM, Strijkers GJ, Drost MR, van Bochove GS, Nicolay K (2007) Skeletal muscle degeneration and regeneration after femoral artery ligation in mice: monitoring with diffusion MR imaging. *Radiology* 243:413–421
16. Steidle G, Schick F (2006) Echoplanar diffusion tensor imaging of the lower leg musculature using eddy current nulled stimulated echo preparation. *Magn Reson Med* 55:541–548
17. Zaraiskaya T, Kumbhare D, Noseworthy MD (2006) Diffusion tensor imaging in evaluation of human skeletal muscle injury. *J Magn Reson Imaging* 24:402–408

-
18. Staron RS, Kraemer WJ, Hikida RS, Fry AC, Murray JD, Campos GE (1999) Fiber type composition of four hindlimb muscles of adult Fisher 344 rats. *Histochem Cell Biol* 111:117–123
 19. Fitts RH, McDonald KS, Schluter JM (1991) The determinants of skeletal muscle force and power: their adaptability with changes in activity pattern. *J Biomech* 24(Suppl 1):111–122
 20. Jarvinen TA, Jozsa L, Kannus P, Jarvinen TL, Jarvinen M (2002) Organization and distribution of intramuscular connective tissue in normal and immobilized skeletal muscles. An immunohistochemical, polarization and scanning electron microscopic study. *J Muscle Res Cell Motil* 23:245–254
 21. Gallagher D, Heymsfield SB (1998) Muscle distribution: variations with body weight, gender, and age. *Appl Radiat Isot* 49:733–734
 22. Janssen I, Heymsfield SB, Wang ZM, Ross R (2000) Skeletal muscle mass and distribution in 468 men and women aged 18–88 years. *J Appl Physiol* 89:81–88